Geometries, Stabilities, and Vibrational Properties of Bimetallic Mo_2-Doped Ge_n ($n = 9-15$) Clusters: A Density Functional Investigation

Jin Wang[†] **and Ju-Guang Han***[,‡]

Department of Chemistry, University of Guelph, Guelph, N1G 2W1, Ontario, Canada, and National synchrotron Radiation Laboratory, University of Science and Technology of China, Hefei 230026, People's Republic of China

Received: October 23, 2007; In Final Form: January 4, 2008

Geometries of the bimetallic Mo_2Ge_n ($n = 9-15$) clusters have been investigated systematically with the density functional approach. The relative stabilities and charge-transfer and vibrational properties of these clusters are presented and discussed. The dominant geometries of Mo_2Ge_n ($n = 9-12$) clusters can be described as one Mo atom inside a Ge cage and another Mo atom on the surface at smaller sizes with $n = 9-12$. Interestingly, the stable geometry of Mo_2Ge_9 cluster has the framework which is analogous to a recent experimental observation (Goicoechea, J. M.; Sevov, S. C. *J. Am Chem. Soc*. **2006**, *128*, 4155). The calculated fragmentation energies and the obtained relative stabilities demonstrate that the remarkable Mo_2-doped Ge_{12} is the most stable species of all different sized clusters. The critical size of Mo_2-encapsulated cagelike germanium clusters appears at $n = 15$. The largest energy gap and strongest stability of Mo_2Ge_{12} enable this species to be a unit of multiple metal Mo-doped germanium nanotubes. Vibrational mode analyses of Mo_2-Ge_n clusters demonstrate that the Mo−Mo stretching vibrations are sensitive to the geometries of the germanium frame, and that the point-group symmetry of germanium clusters can vary the Mo−Mo stretching vibration relative to the IR inactive vibration.

1. Introduction

Recent experimental and theoretical findings of single metal-doped silicon clusters have revealed that the doped transition metal (TM) atom can efficiently enhance the stability of pure silicon clusters. The TM-doped silicon and germanium clusters exhibit a variety of geometrical arrangement and electronic properties and contribute to generating novel silicon-based nanoscale device components.[1−16] According to some recent investigations, germanium clusters are currently of great interest because metal-encapsulated caged germanium clusters have large highest occupied molecular orbital-lowest unoccupied molecular orbital (HOMO−LUMO) gaps and different growth behaviors compared to the silicon clusters.[17−21] However, no systematic investigations on the growth pattern mechanism for multiple metal-doped silicon and germanium nanotubes evolving in small single metal-doped silicon or germanium clusters have been performed until now. Especially, it is quite important to study the behaviors of transition metal dimer-doped germanium clusters because the bimetallic-doped cagelike germanium clusters are initial models of the multiple metal-doped germanium nanotubes. By aid of the detailed investigation on the interactions between the Mo−Mo dimer and pure germanium clusters, some valuable information, e.g., frontier orbital energy gaps and charge populations of Mo−Mo dimer, etc., is helpful for revealing feasibility on formation of the multiple metal-doped germanium nanotubes. Therefore, in order to compare different behaviors between the Mo−Mo-doped germanium clusters and single TM atom-doped germanium clusters,[22] present investigations mainly focus on the growth pattern behaviors and electronic properties of the Mo_2-doped cagelike germanium clusters at the size from 9 to 15, which can provide significant assistance in the quest for such kinds of cluster-assembled materials.

2. Computational Details

In order to provide accurate and reliable results, the geometry optimizations of the bimetallic Mo_2-doped Ge_n clusters are performed by using density functional theory (DFT) with the unrestricted B3LYP exchange-correlation potential and an effective core potential LanL2DZ basis sets.[22−27] The standard LanL2DZ basis sets can provide an effective way to reduce difficulties in calculations of two-electron integrals caused by heavy transition metal Mo atoms. All computational works are carried out by Gaussian 03 package.[26]

For clusters containing 12−18 atoms being considered, there are a very large number of local minima for each size at the DFT level, and it is not likely that the small subset chosen contains the best structures. Therefore, in this article we try to examine if the localization of Mo atoms upon/into germanium clusters causes the major rearrangement of the geometrical framework of Ge_n clusters (or cages) as well as to explore the striking changes in the properties of Ge_n clusters due to the insertion of the various transition metals. The strategy of searching the possible Mo_2Ge_n geometries with different evolvement patterns can be organized as follows: (1) On the basis of our previous thoretical investigations on the single TM (TM = Cu, Ni, and Zn) atom-doped germanium isomers,[18,19,22,27] one Ge atom in the small-sized single TMA-doped germanium clusters is replaced by the second new Mo atom. (2) The bimetal Mo_2 being directly inserted into the pure germanium cages.

* To whom correspondence should be addressed. E-mail: jghan@ustc.edu.cn or jwang02@uoguelph.ca.
[†] University of Guelph.
[‡] University of Science and Technology of China.

10.1021/jp710238t CCC: $40.75 © 2008 American Chemical Society
Published on Web 03/05/2008

TABLE 1: The Calculated Bond Length (Å), Atomic Dissociation Energy (eV/atom), Frequency (cm^{-1}), and Electronic State for the Ge_2, Mo_2, and MoGe Dimers

clusters	method	bond length (Å)	dissoation energy (eV)	freq (cm^{-1})	electronic state
Ge_2	B3LYP	2.53	1.17	171.4	$^3\sum_{g'}$
	B3LYP[a]	2.55			$^3\sum_{g'}$
GeMo	B3LYP	2.50	1.34	208.1	
Mo_2	B3LYP	1.98	1.8	562.0	$^1\sum$
	B3LYP[b]	1.98	1.8	562.0	$^1\sum^+_g$
	LSDA[c]	1.95	2.17	520.0	$^1\sum^+_g$
	EXP[d]	1.94	2.19	477.0	$^1\sum^+_g$

[a] Reference 16. [b] Reference 31. [c] Reference 28. [d] Reference 29.

(3) One germanium atom being surface capped on the small-sized Mo_2Ge_{n-m} clusters. (4) Rearrangement the geometries or deduced symmetries of the Mo_2Ge_n isomers with high symmetries.

Our previous investigations on the single TMA-doped silicon or germanium clusters at the UB3LYP/LanL2DZ level are proven to be reliable.[16,18,19,27] To test the reliability of our calculations, the respective Ge_2, Mo_2, and MoGe molecules are carried out, and the calculated bond lengths, vibrational frequencies, and dissociation energies are illustrated in Table 1. From Table 1, one finds that the calculated results of Ge_2, Mo_2, and MoGe clusters are in good agreement with the reported theoretical and experimental results that are available.[28,29,31] This examination of equilibrium bond lengths and angles leads to deviations typically within 1−6%. Since the calculated results also depend on the pseudopotentials, our study can be considered as preliminary and qualitative in nature.

In addition, the spin state effect is considered also and the calculated results of Mo_2Ge_n isomers indicate that the total energies of the triplet and quintet spin states are higher than that of singlet spin state. The spin contamination for all transition-metal Mo_2-doped germanium clusters is calculated. The spin contamination for the most stable geometries is zero and will not be discussed in this paper. In addition, the comparisons with the previous theoretical results of TM (TM = Cu, Ni, and Zn)-doped germanium clusters are made.[18,19,27]

3. Results and Discussions

3.1. Geometries and Stabilities of Mo_2Ge_n (n = 9−12). A variety of possible initial geometries of Mo_2Ge_9 isomers are considered, and eight stable isomers have been obtained after the geometries were optimized. Except for the **9h** isomer, all the other stable structures can be described as the Mo-encapsulated and Mo-capped species, i.e., one Mo atom is encapsulated into the caged Ge_9 framework and the other Mo atom is capped on the surface of the formed $MoGe_9$ framework. One tricapped trigonal prism (TTP) **9f** with the bimetallic Mo−Mo dimer (Figure S1) that is parallel inserted into the germanium frame is optimized as a minimum, which is analogous to the experimental Ni_2Ge_9 geometry and can be described as one Mo being surface capped on the antiprism $MoGe_9$ frame.[2,30] The distance of Mo−Mo bond length is elongated after the bimetallic Mo−Mo dimer is inserted into the Ge_9 framework. Although the TTP **9f** is proven to be a stable structure, it is not the lowest-energy geometry of all the eight Mo_2Ge_9 isomers, which is analogous to the Mo_2Si_9 geometry.[31] The low-lying **9b** and **9d** geometries, which are shown in Figure S1, are described as the bimetallic Mo−Mo dimer being inserted into the bisquare germanium prisms. Previous experimental results demonstrated that the bicapped square antiprism is a common structure motif for the empty nine-atom clusters that

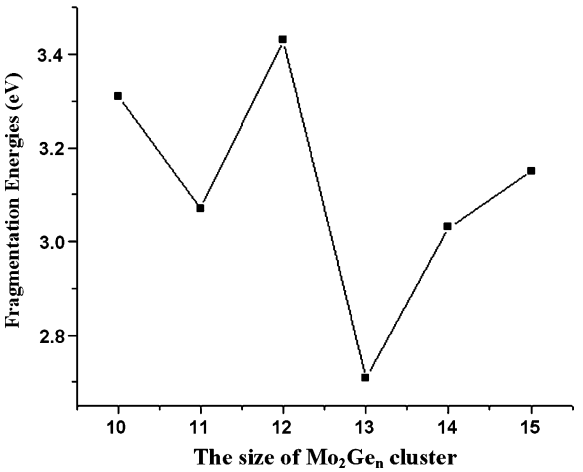

Figure 1. Sized dependence of the fragmentation energies of the most stable Mo_2Ge_n clusters.

are capped by transition-metal complex fragments.[32,33] As far as the Mo_2Ge_9 **9h** cluster is concerned, the stability of the bimetallic Mo−Mo concaved nine-atom germanium cage is quite weakened, reflecting that the total energy of **9h** isomer is obviously higher as compared to that of others with one Mo atom being capped on the $MoGe_9$ frame after one Mo atom is encapsulated into the Ge_9 germanium frame (Table 2), and that the encapsulated Mo atom tries to terminate all the dangling bonds of all the germanium atoms. The most stable Mo_2Ge_9 isomer is slightly deviated relative to the $TMGe_9$ (TM = Cu and Ni) geometries;[18,19] however, it seriously deformed the WGe_9 geometry.[27]

As far as the Mo_2Ge_{10} cluster is concerned, the low-lying **10a** and **10b** isomers have different geometries. The **10a** isomer is formed by the bimetallic Mo−Mo being vertically inserted into the pentagonal germanium prism while the **10b** isomer is formed by the Mo−Mo dimer being inserted into the bicapped square prism. Although the calculated total energies of these two isomers are slightly different (Table 2), the **10a** isomer is selected as the possible candidate of the ground state. Previous theoretical investigations indicated that the single-TMA-encapsulated pentagonal prism Ge_{10} does not dominate the growth pattern, and the formed species is much higher in total energy than the TMA-encapsulated tetragonal antiprism isomers.[18,19] However, detailed studies of the bimetallic Mo−Mo-doped germanium clusters reveal that the most stable species of the Mo_2Ge_{10} cluster is also formed by the Mo−Mo dimer being vertically inserted into the pentagonal germanium prism, which is analogous to the lowest-energy Mo_2Si_{10} cluster in geometry;[31] however, it is different from the geometries of $CuGe_{10}$, $NiGe_{10}$, and WGe_{10} clusters.[18,19,27] As shown in Figure S1 and Table 2, the **10d** isomer, which is formed by the Mo−Mo dimer being parallel inserted into the bipentagonal germanium prisms, is higher in total energy by 0.91 eV than the lowest-energy **10a** isomer which is obtained after the Mo−Mo dimer is vertically inserted into pentagonal germanium prisms. It should be pointed out that the growth pattern of the bimetallic Mo−Mo dimer vertically doped germanium is superior to that of the Mo−Mo parallel doped pentagonal germanium prisms. The Mo−Mo dimer-concaved Mo_2Ge_{10} isomers (**10c**, **10f,** and **10g**) have been identified; however, they are not the dominant growth pattern because their total energies are relatively higher as compared to those of **10a** and **10b** isomers.

Guided by the lowest-energy Mo_2Ge_{10} **10a** cluster, the most stable Mo_2Ge_{11} **11a** isomer, which is also based on pentagonal germanium prisms with the eleventh germanium atom being

TABLE 2: Geometries, Total Energies of the Mo_2Ge_n ($n = 9-12$) Clusters

cluster	symmetry	freq[a] (cm^{-1})	state[b]	Mo−Mo[c] (Å)	E_T[d] (hartree)	relative energy (eV)
Mo_2Ge_9	C_1 (a)	12.8	^1A	2.449	−169.1238447	
	C_s (b)	47.7	^1A	2.358	−169.1161307	0.21
	C_s (c)	34.3	^1A	2.492	−169.1157044	0.22
	C_s (d)	36.1	^1A	2.486	−169.1048771	0.52
	C_1 (e)	35.8	^1A	2.423	−169.1040433	0.54
	C_{3v} (f)	37.0	$^1A1$	2.551	−169.1028496	0.57
	C_1 (g)	37.5	^1A	2.430	−169.0897891	0.93
	C_1 (h)	36.6	^1A	2.482	−169.0754379	1.32
Mo_2Ge_{10}	C_1 (a)	34.5	^1A	2.461	−172.9227917	
	C_s (b)	45.8	^1A	2.402	−172.9200319	0.08
	C_s (c)	46.8	^1A	2.478	−172.9001657	0.62
	C_1 (d)	31.9	^1A	2.413	−172.8894668	0.91
	C_1 (e)	37.0	^1A	2.447	−172.8859323	1.01
	C_1 (f)	29.0	^1A	2.438	−172.8835322	1.07
	C_s (g)	40.3	^1A	2.596	−172.8690211	1.46
Mo_2Ge_{11}	C_1 (a)	33.3	^1A	2.429	−176.7130009	
	C_1 (b)	27.8	^1A	2.409	−176.7013684	0.32
	C_1 (c)	32.7	^1A	2.384	−176.6874040	0.70
	C_1 (d)	29.2	^1A	2.535	−176.6830110	0.82
	C_1 (e)	20.0	^1A	2.489	−176.6829014	0.82
	C_1 (f)	33.7	^1A	2.467	−176.6808335	0.88
	C_1 (g)	23.4	^1A	2.522	−176.6804316	0.89
	C_1 (h)	33.9	^1A	2.593	−176.6802046	0.89
	C_1 (i)	17.8	^1A	2.462	−176.6756623	1.02
	C_1 (k)	32.0	^1A	2.392	−176.6633993	1.35
Mo_2Ge_{12}	C_1 (a)	29.7	^1A	2.360	−180.5164639	
	C_1 (b)	38.7	^1A	2.403	−180.5059294	0.29
	C_1 (c)	30.8	^1A	2.415	−180.4991345	0.47
	C_1 (d)	28.0	^1A	2.576	−180.4803348	0.98
	C_1 (e)	33.7	^1A	2.582	−180.4778786	1.05
	C_1 (f)	45.8	^1A	2.616	−180.4737508	1.16
	C_1 (g)	29.7	^1A	2.620	−180.4730759	1.18
	C_1 (h)	36.7	^1A	2.294	−180.4576512	1.60
	C_1 (i)	33.7	^1A	2.662	−180.4546776	1.68
	C_1 (k)	21.7	^1A	2.507	−180.4377176	2.14

[a] Freq denotes the lowest vibrational frequency. [b] State represents electronic state. [c] Mo−Mo represents Mo−Mo bond length. [d] E_T represents the total energies of different isomers.

added, is yielded. Ten different Mo_2Ge_{11} isomers are mainly divided into two kinds of isomers, i.e., Mo capped on Mo-encapsulated germanium cages (**11a**−**11c** etc.), and Mo−Mo-concaved germanium cages (**11d**, **11e,** and **11h**, etc.). It is worth pointing out that the **11a** geometry is different from that of Mo_2Si_{11} and $TMGe_{11}$ clusters (TM = Cu, Ni, and W).[18,19,27]

The optimized geometries indicate that the possible Mo_2Ge_{12} isomers with high symmetries are not the stable structures. Interestingly, the most stable Mo_2Ge_{12} isomers can be identified as one Mo atom being capped on the Mo-encapsulated hexagonal anti-prism C_6 Ge_{12} **12a** (Figure S1). Furthermore, a variety of possible isomers are checked and optimized, which have been found as the low-lying Mo_2Ge_{12} isomers. On the basis of the calculated total energies of the stable Mo_2Ge_{12} isomers, they demonstrate that the Mo−Mo parallel inserted hexagonal anti-prism Mo_2Ge_{12} **12a** with the Mo−Mo dimer acting as a symmetrical axis is the most stable because it has the lowest total energy as compared to all the other isomers (Table 2). It can be expected that the hexagonal anti-prism Mo_2Ge_{12} geometry is an important building block of multiple metal Mo-doped germanium-based nanotubes. Furthermore, the most stable **12a** isomer has a geometrical framework analogous to that of the Mo_2Si_{12} cluster;[31] however, it is quite different from the geometries of the most stable basketlike TM (TM = W, Ni, and Cu)-doped germanium clusters.[18,19,27]

3.2. Geometries and Stabilities of Mo_2Ge_n ($n = 13-15$) Clusters. As mentioned above, the Mo_2 inserted hexagonal anti-prism Mo_2Ge_{12} **12a** cluster is the lowest-energy isomer. On the basis of the **12a** geometry, the most stable Mo_2Ge_{13} isomer can be depicted as the thirteenth Ge atom being capped on the hexagonal anti-prism Mo_2Ge_{12} cluster and the second Mo atom being concaved on the germanium framework. It should be mentioned that the dominant growth behavior of the bimetallic Mo_2-doped Ge_n clusters begins to vary from one Mo atom being capped on the other Mo atom-encapsulated germanium framework to one Mo atom being concaved on the other Mo atom-encapsulated germanium frame, which is reflected from a variety of the stable Mo_2Ge_{13} geometries at the size of **13**, except for the **13c** isomer. It should be mentioned that the stability of **13c** isomer is remarkably weaker than that of the lowest-energy **13a** isomer in that the total energy of the former is distinctly higher than that of the latter by 0.33 eV (Figure S2 and Table 3). The most stable Mo_2-doped Ge_{13} geometry, which is analogous to the geometry of the Mo_2-doped Si_{13} cluster,[31] deviates slightly from that of WGe_{13} cluster.[27] However, it is different from that of $TMGe_{13}$ (TM = Cu, Ni, and Zn) clusters.[18,19,22]

The bimetallic Mo_2 vertically inserted pentagonal Ge_{14} prism contributes to formation of the layered structure. As shown in Figure S2, the second Mo atom in the lowest-energy **14a** structure is concaved on the second layer of germanium framework, revealing that the bimetallic Mo−Mo-doped double layers of the open-caged germanium framework begin to be formed. Additionally, the tetracapped germanium atoms capped on the pentagonal prism Mo_2Ge_{10} **10a** cluster also form the almost isoenergetic low-lying **14b** isomer. On the other hand, the bimetallic Mo−Mo parallel inserted bipentagonal prism Mo_2Ge_{10} **10d** is helpful for forming the layered structure. As shown in Figure S2, the **14f** isomer has one Mo atom inserted into the bipentagonal prism Ge_{10} frame and the second Mo atom is encapsulated into the bisquare prism. As mentioned before, the

TABLE 3: Geometries, Total Energies of the Mo_2Ge_n ($n = 13-15$) Clusters

cluster	symmetry	freq[a] (cm^{-1})	state[b]	Mo−Mo[c] (Å)	E_T[d] (hartree)	relative energy (eV)
Mo_2Ge_{13}	C_1 (a)	20.4	^1A	2.397	−184.2932883	
	C_1 (b)	29.1	^1A	2.409	−184.2843978	0.24
	C_1 (c)	36.3	^1A	2.413	−184.2812681	0.33
	C_1 (d)	16.5	^1A	2.575	−184.2800362	0.36
	C_s (e)	21.5	^1A	2.565	−184.2707358	0.61
	C_1 (f)	32.8	^1A	2.651	−184.2694190	0.65
	C_1 (g)	39.1	^1A	2.579	−184.2639546	0.80
	C_1 (h)	35.8	^1A	2.460	−184.2628970	0.83
	C_1 (i)	19.5	^1A	2.565	−184.2464619	1.27
	C_1 (k)	19.4	^1A	2.595	−184.2386334	1.49
	C_s (l)	19.5	$^1A'$	2.685	−184.2290079	1.75
Mo_2Ge_{14}	C_1 (a)	13.8	^1A	2.475	−188.0818708	
	C_1 (b)	45.1	^1A	2.414	−188.0817492	0.003
	C_1 (c)	30.3	^1A	2.397	−188.0724527	0.26
	C_1 (d)	47.2	^1A	2.458	−188.0716616	0.28
	C_1 (e)	31.5	^1A	2.446	−188.0695557	0.34
	C_1 (f)	34.2	^1A	2.644	−188.0648480	0.46
	C_s (g)	37.9	$^1A'$	2.601	−188.0610585	0.57
	C_1 (h)	15.8	^1A	2.542	−188.0561651	0.70
	C_s (i)	29.2	^1A	2.847	−188.0221264	1.63
Mo_2Ge_{15}	C_1 (a)	38.0	^1A	2.516	−191.8748793	
	D_5 (b)	27.1	$^1A_1$	2.495	−191.8720497	0.08
	C_1 (c)	14.7	^1A	2.590	−191.8712145	0.10
	C_s (d)	17.5	$^1A'$	2.590	−191.8688773	0.16
	C_1 (e)	37.6	^1A	2.456	−191.8670357	0.21
	C_1 (f)	8.70	^1A	2.571	−191.8663725	0.23
	C_1 (g)	26.3	^1A	2.645	−191.8633885	0.31
	C_1 (h)	21.1	^1A	2.663	−191.8620915	0.35
	C_1 (i)	27.2	^1A	2.837	−191.8583155	0.45
	C_1 (k)	14.5	^1A	2.537	−191.8508506	0.65
	C_1 (l)	40.4	^1A	2.461	−191.8429722	0.87

[a] Freq denotes the lowest vibrational frequency. [b] State represents the electronic state. [c] Mo−Mo represents the Mo−Mo bond length. [d] E_T represents the total energies of different isomers.

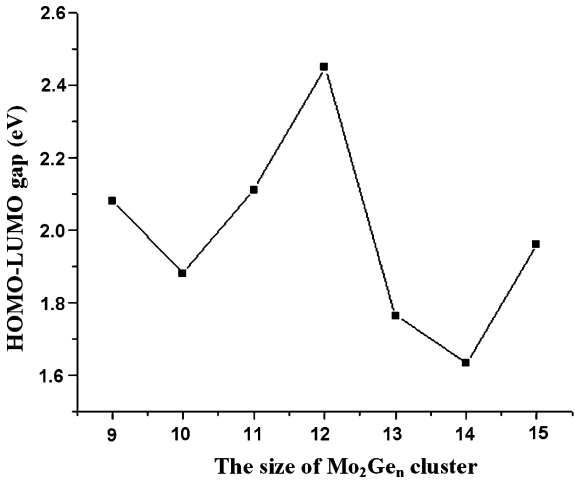

Figure 2. Sized dependence of HOMO−LUMO gap of the most stable Mo_2Ge_n clusters.

bimetallic Mo−Mo parallel-doped growth pattern is inferior to the Mo−Mo vertically doped growth pattern, and the total energy of **14f** is higher than that of **14a** by 0.46 eV. It should be mentioned that the Mo_2-doped Ge_{14} geometry is slightly different from the geometrical framworks of Mo_2Si_{14} and WGe_{14} clusters,[27,31] and that the transition metal Mo and W atoms in the Mo_2Si_{14} and WGe_{14} isomers are completely encapsulated into the respective silicon or germanium frames at the size of $n = 14$.

With respect to the Mo_2Ge_{15} clusters, two low-lying **15a** and **15b** isomers have been found as the stable structures, and it is demonstrated that the bimetallic Mo−Mo parallel-encapsulated double-layered sealed cagelike empty germanium structure can be formed. According to the optimized stable Mo_2Ge_{15} geometries, one finds that the dominant Mo_2-doped Ge_n growth pattern begins to vary from one Mo atom being concaved on the other Mo-encapsulated germanium cage to the bimetallic Mo−Mo being completely encapsulated into the closed germanium cage. It is interesting that the Mo_2Ge_n clusters undergo a structural transition at $n = 15$. It should be pointed out that the bimetallic Mo_2 dimer-doped fullerene-like germanium geometries are not the dominant growth pattern because the fullerene-like Mo_2Ge_{15} **15k** is higher in total energy by 0.65 eV than that of the double-layered most stable **15a** isomer. It is worth pointing out that the most stable **15a** geometry is analogous to that of Mo_2Si_{15} cluster;[31] however, it is different from the geometry of WGe_{15} cluster.[27]

It should be mentioned that the encapsulated Mo atoms in the most stable Mo_2Ge_n ($n = 9-16$) clusters obtain more charges from their surroundings than that of the surface-capped Mo atom, and that the encapsulated Mo atom has a tendency to interact with more germanium atoms with unequivalent bond lengths and to terminate the dangling bonds of germanium atoms. Therefore, the doped Mo atoms play very important roles in the stabilities of the Mo_2-doped Ge_n ($n = 9-15$) clusters. Theoretical investigation on the slightly deformed low-lying C_{7v} Mo_2Si_{14}, C_{8v} Mo_2Si_{16}, Mo_2Ge_n clusters indicates that the Mo-doped Si_n can form the nanotube easily[31] and the Mo-doped Ge_n clusters do not easily form the stable nanotube.

3.3. The Relative Stabilities. According to the calculated fragmentation energy of different sized clusters, the valuable information of their relative stabilities can be obtained. The fragmentation energy of the Mo_2Ge_n ($n = 9-15$) clusters is defined as:

$$D(n, n-1) = E_T(Mo_2Ge_{n-1}) + E_T(Ge) - E_T(Mo_2Ge_n)$$

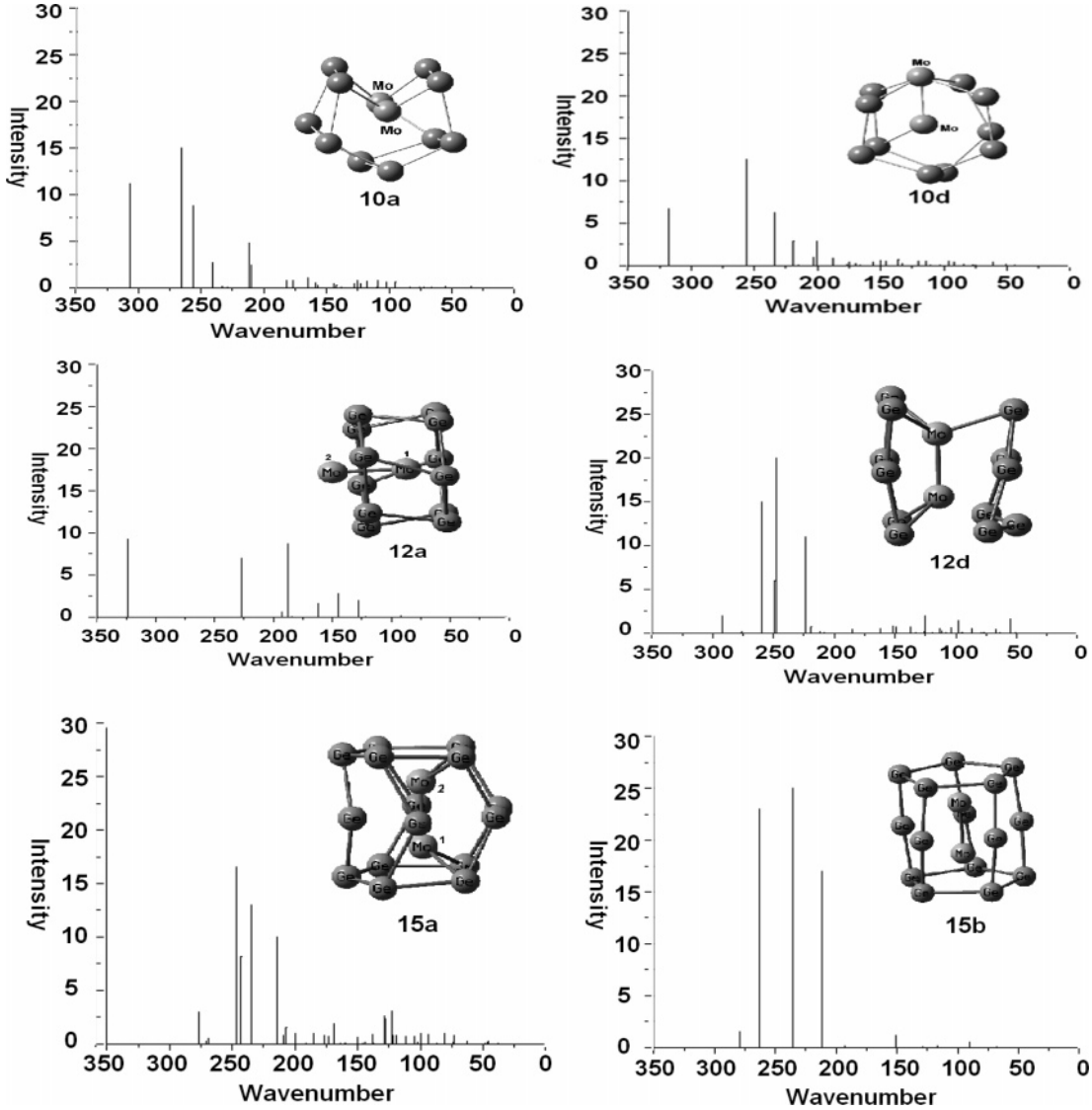

Figure 3. Infrared vibrational spectra of different sized clusters: Mo_2Ge_{10} (**10a** and **10d**), Mo_2Ge_{12} (**12a** and **12b**), and Mo_2Ge_{15} (**15a** and **15b**). Intensities are presented in Km/mol and wavenumber in cm^{-1}.

On the basis of the calculated fragmentation energies, which are shown in Figure 1, the remarkable maximum for the Mo_2Ge_n ($n = 9-15$) clusters appearing at $n = 12$ has been found. It indicates that the corresponding cluster has relatively stronger stability as compared to its neighbors (Figure 1). This finding is similar to that of Mo_2Si_{12} cluster.[31] The lowest-energy geometries from Mo_2Ge_{14} to Mo_2Ge_{15} with a gradually increased relative stability with the size of clusters are based on the double-layered pentagonal prism, which supports the conclusion that the bimetallic Mo−Mo vertically doped pentagonal prism Mo_2Ge_{10} is a possible model of multiple metal-doped germanium nanotubes as discussed previously.

3.4. The HOMO−LUMO Gap and Charge-Transfer Mechanisms. The HOMO−LUMO gaps of different sized bimetallic germanium clusters are illustrated at Table 3 and shown in Figure 2. On the basis of the calculated results, one finds that the HOMO−LUMO gap of Mo_2Ge_{12} cluster is quite higher in comparison with the other sized clusters (Figure 2). As mentioned above, the fragmentation energy of Mo_2Ge_{12} is remarkably higher than its neighbor species. The large fragmentation and energy gap of the Mo_2Ge_{12} cluster indicate that its chemical stability is relatively stronger as compared to its adjacent sized cluster; this finding is similar to that of Mo_2Si_{12} cluster.[31] Moreover, the large HOMO−LUMO gap (2.449 eV) of Mo_2Ge_{12} makes this cluster a luminescent material in the blue region. Hence, the large HOMO−LUMO gap and the enhanced stability of Mo_2Ge_{12} make it behave as superatoms. It can be expected that the enhanced stability of Mo_2Ge_{12} makes a contribution toward the initial model for formation of a new type of multiple Mo-doped germanium nanotubes. In other words, the Mo_2Ge_{12} cluster can be described as two $MoGe_6$ or $(MoGe_6)_2$ units. The new type Mo-doped germanium nanotube is described as the $((MoGe_6)_n$ form with a large size of n.

In order to investigate charge transfer between the Mo−Mo dimer and germanium frames, natural population analyses for the different sized clusters are performed. As illustrated in Table 4, more negative charges for the lowest-energy Mo_2Ge_n ($n = 9-13$) isomers are localized at the encapsulated Mo atom as compared to the capped Mo atom at different sized clusters (Table 4). However, the negative charges for the lowest-energy Mo_2Ge_{14} and Mo_2Ge_{15} isomers are also identically localized at the Mo_2 atoms. These findings are similar to those of the Mo_2Si_n ($n = 9-15$) clusters.[31] It is interesting that the balanced negative charge being localized at the bimetal Mo−Mo dimer of the caged Mo_2Ge_{15} (**15a** and **15b**) clusters efficiently dissipates the excess charges of the empty germanium cages.

TABLE 4: The HOMO−LUMO Gaps and Natural Charge Populations of the Lowest-Energy Mo_2Ge_n Clusters

clusters	HOMO (hartree)	LUMO (hartree)	HOMO−LUMO gap (eV)	natural charge population
Mo_2Ge_9	−0.2077	−0.1313	2.081	Mo(1) −1.582 Mo(2) −0.458
Mo_2Ge_{10}	−0.2033	−0.1341	1.881	Mo(1) −1.504 Mo(2) −0.478
Mo_2Ge_{11}	−0.2112	−0.1336	2.111	Mo (1) −1.443 Mo(2) −0.471
Mo_2Ge_{12}	−0.2125	−0.1225	2.449	Mo (1) −1.275 Mo(2) −0.291
Mo_2Ge_{13}	−0.1971	−0.1322	1.764	Mo (1) −1.346 Mo (2) −0.621
Mo_2Ge_{14}	−0.2116	−0.1516	1.632	Mo (1) −1.684 Mo (2) −1.594
Mo_2Ge_{15}	−0.2124	−0.1403	1.961	Mo (1) −1.486 Mo (2) −1.486

The dangling bonds of germanium atoms of Mo_2Ge_{15} (**15a** and **15b**) clusters can be obviously terminated by the Mo−Mo dimer, and the interactions between the Mo−Mo dimer and the germanium atoms enhance the stability of the Mo_2-doped cagelike Ge_{15} clusters, reflecting that the germanium cages or clusters are easily formed under the interactions of bimetal Mo_2 and the germanium frame after the Mo_2 dimer is encapsulated into the germanium frame. Moreover, the Mo−Mo dimer contributes to the transformation of the bonding type of germanium atoms from sp^3 to sp^2 hybridization.

3.5. Vibrational Properties of Different Sized Mo_2Ge_n Clusters. Recently, one new technology of FELIX (free electron laser for infrared experiment) is successfully applied for the investigations on vibrational infrared spectra of neutral transition metal-doped carbide clusters.[33] It is important for us to preliminarily analyze vibrational properties of different sized Mo_2Ge_n clusters now so that some valuable information of different vibrational modes of these clusters can be provided.

Vibrational frequency analyses of several typical Mo_2Ge_n clusters are performed, and theoretical infrared spectra of these clusters are given in Figure 3. In the case of the Mo_2Ge_{10} cluster, the Mo−Mo parallel and vertically doped empty pentagonal prism cagelike Ge_{10} cluster results in the formation of two isomers **10a** and **10d**. As seen from their infrared spectra which is shown in Figure 3, the localization and intensity of the Mo−Mo stretching vibration mode in the two isomers above are obviously different; that is, the Mo−Mo stretching vibrational band in the **10a** isomer appears at 307 cm^{-1}. However, this vibrational mode in the **10d** isomer is shifted toward to 318 cm^{-1}, and its intensity is relatively decreased as compared to the **10a** isomer. As far as the **10a** and **10d** isomers are concerned, the strongest vibrational bands appear at 266 and 256 cm^{-1}, respectively, and vibrational modes can be assigned as Mo−Ge stretching vibrations.

In the case of the Mo_2Ge_{12} clusters, vibrational frequency analyses of two typical isomers **12a** and **12d** are investigated because the **12a** geometry with one capped Mo atom and another encapsulated Mo atom is formed in contrast to the **12d** geometry with one concaved Mo atom and other encapsulated Mo atom. As shown in Figure 3, the Mo−Mo stretching vibration intensity in **12d** is quite weak and its vibrational band appears at 276 cm^{-1}; thus, it is not shown at its theoretical infrared spectrum. On the contrary, the Mo−Mo stretching vibration intensity of **12a** is stronger, which appears at 323 cm^{-1}. It should be mentioned that the strong vibrational band at 227 cm^{-1} in **12a** is generated from two degenerate sketching stretches of the encapsulated Mo atoms and hexagonal anti-prism Ge_{12} cage.

As discussion before, the low-lying Mo_2Ge_{15} isomers **15a** and **15b** are almost isoenergetic species, and they belong to the two-layer pentagonal prism structure; however, the **15b** has D_5 point-group symmetry which is different from that of **15a** isomer. As seen from their infrared vibrational spectra (Figure 3), the infrared spectrum of **15a** is much more complicated than that of **15b**. Interestingly, the Mo−Mo stretching vibration at 284 cm^{-1} for **15b** is infrared inactive because the alteration of dipole moment of this vibrational mode is completely dispelled by symmetrical two-layer pentagonal prism of the germanium cage. On the other hand, the Mo−Mo stretching vibration at 277 cm^{-1} in **15a** is infrared active; meanwhile its intensity is quite weak. Compared to infrared spectra of **15a**, three predominant vibrational bands of **15b** appear at 263 cm^{-1}, 235 cm^{-1}, and 212 cm^{-1}, respectively, and they can be assigned as asymmetric stretching vibrations between the Mo−Mo dimer and the caged germanium frame.

4. Conclusions

Investigations on the geometries and stabilities of the bimetallic Mo_2Ge_n ($n = 9-15$) clusters as well as other properties such as energy gaps and vibrational properties have been carried out by using the UB3LYP/LanL2DZ method. All the calculated results can be summarized as follows: (1) The most stable Mo_2Ge_n ($n = 9-13$) isomers feature one Mo atom inside a Ge cage and another Mo atom on the surface at smaller cluster sizes. When the cluster size increases to 15, the dominant structures have the Mo−Mo dimer completely encapsulated into the germanium clusters. (2) The largest energy gap and strongest stability of Mo_2Ge_{12} **12a** make this species a unit of multiple metal-doped germanium nanotubes. The formation of the stable double-layer pentagonal prism Mo_2Ge_{15} (**15a** and **15b**) reflects that new quasi-one-dimentional Mo−Ge nanotubes based on pentagonal prism are possible. (3) Analyses of vibrational properties of the Mo−Mo-doped germanium clusters indicate that the Mo−Mo stretching vibrations are sensitive to the germanium cage and that the geometrical symmetry of caged structures can vary the infrared active Mo−Mo vibrational stretch modes to the infrared inactive Mo−Mo vibrational stretch modes. Moreover, infrared spectra contribute to identification and characterization of the Mo_2Ge_n species if the FELIX technology is available. In additon, the growth pattern of the most stable Mo_2Ge_n ($n = 9-15$) clusters deviates slightly relative to that of the Mo_2Si_n ($n = 9-15$) clusters.[31]

Acknowledgment. This work is supported by the National Science Fund (985029) and NSERC foundation of Canada. The author (H.J.G.) thanks Dr. R. N. Zhao for her significant discussions and modifications.

Supporting Information Available: Equilibrium geometries of the Mo_2Ge_n clusters. This material is available free of charge via the Internet at http://pubs.acs.org.

References and Notes

(1) Beck, S. M. *J. Chem. Phys.* **1987**, *87*, 4233.
(2) Beck, S. M. *J. Chem. Phys.* **1989**, *90*, 6306.
(3) Lu, J.; Nagase, S. *Phys. Rev. Lett.* **2003**, *90*, 115506.
(4) Han, J. G.; Shi, Y. Y. *Chem. Phys.* **2001**, *266*, 33.
(5) Sen, P.; Mitas, L. *Phys. Rev. B* **2003**, *68*, 155404.
(6) Han, J. G. *Chem. Phys.* **2003**, *286*,181.
(7) Han, J. G.; Hagelberg, F. *Chem. Phys.* **2001**, *263*, 255.
(8) Gueorguiev, G. K.; Pacheco, J. M. *J. Chem. Phys.* **2003**, *119*, 10313.
(9) Han, J. G.; Hagelberg, F. *Comput. Lett.* **2005**, *1*, 230.

(10) Hiura, H.; Miyazaki, T.; Kanayama, T. *Phys. Rev. Lett.* **2001**, *86*, 1733.
(11) Ohara, M.; Miyajima, K.; Pramann, A.; Nakajima, A.; Kaya, K. *J. Phys. Chem. A.* **2002**, *106*, 3702.
(12) Zhao, R. N.; Ren, Z. Y.; Guo, P.; Bai, J. T.; Zhang, C. H.; Han, J. G. *J. Phys. Chem. A* **2006**, *110*, 4071.
(13) Miyazaski, T.; Hirua, H.; Kanayama, T. *Phys. Rev. B* **2002**, *66*, 121403.
(14) Chen, Z. F.; Neukermans, S.; Wang, X.; Janssens, E.; Zhou, Z.; Silverans, R. E.; King, R. B.; Schleyer, P. V.; Lievens, P. *J. Am. Chem. Soc.* **2006**, *128*, 12839.
(15) Wang, J.; Han, J. G. *J. Chem. Phys.* **2005**, *123*, 064306.
(16) Han, J. G.; Ren, Z. Y.; Lu, B. Z. *J. Phys. Chem. A* **2004**, *108*, 5100.
(17) Wang, J.; Han, J. G. *J. Chem. Phys.* **2005**, *123*, 244303.
(18) Wang, J.; Han, J. G. *J. Phys. Chem. B* **2006**, *110*, 7820.
(19) Han, J. G. *J. Comput. Theoret. Nanosci.*, submitted.
(20) Singh, A. K.; Kumar. V.; Kawazoe, Y. *Phys. Rev. B* **2005**, *71*, 075312.
(21) Wang, J.; Han, J. G. *Chem. Phys*. **2007**, *342*, 253.
(22) Becke, A. D. *Phys. Rev. A* **1988**, *38*, 3098.
(23) Lee, C.; Yang, W.; Parr, R. G. *Phys. Rev. B* **1988**, *27*, 785.
(24) Wadt, W. R.; Hay, P. J. *J. Chem. Phys.* **1985**, *82*, 284.
(25) Frish, M. J. et. al. *Gaussian03*, Gaussian Inc., Pittsburgh, PA, 2003.
(26) Wang, J.; Han, J. G. *J. Phys. Chem. A* **2006**, *110*, 12670.
(27) Delley, B.; Freeman, A.; Ellis, D. E. *Phys. Rev. Lett*. **1983**, *50*, 488.
(28) Morse, M. D. *Chem. Rev.* **1986**, *86*, 1049.
(29) Goicoechea, J. M.; Sevov, S. C. *J. Am. Chem. Soc.* **2006**, *128*, 4155.
(30) Han, J. G.; Zhao, R. N.; Duan, Y. H. *J. Phys. Chem. A* **2007**, *111*, 2148.
(31) Kesanli, B.; Fettinger, J.; Eichhorn, B. *Chem. Eur. J.* **2001**, *7*, 5277.
(32) Campbell, J.; Mercier, H. P. A.; Holger, F.; Santry, D.; Dixon, D. A.; Schrobilgen, G. J. *Inorg. Chem.* **2002**, *41*, 86.
(33) Heijnsbergen, D. V.; Fielicke. A.; Meijer, G.; Helden. G. V. *Phys. Rev. Lett.* **2002**, *89*, 013401.